The Effects of Turbulent Inflow Condition on Feedback-loop Mechanism in Supersonic Cavity Flows

o Weipeng Li, University of Tokyo, 7-3-1 Hongo, Bunkyo-ku, Tokyo, li@flab.isas.jaxa.jp
Taku Nonomura, ISAS/JAXA, 3-1-1, Yoshinodai, Sagamihara, Kanagawa, 252-5210
Kozo Fujii, ISAS/JAXA, 3-1-1, Yoshinodai, Sagamihara, Kanagawa, 252-5210

The effects of turbulent inflow condition on feedback-loop mechanism are numerically studied by implicit large-eddy simulations of supersonic flows over a cavity under two turbulent-boundary-layer-profiled inflow conditions with fluctuations (TurBL-flu case) and without fluctuations (TurBL-ave case). Results show that higher-speed recirculation flows and high pressure distributions are observed in the TurBL-flu case. The behaviors of the shear-layer in these two cases are much different. Two-dimensional shedding vortices in spanwise are clearly observed in the shear-layer of the TurBL-ave case, while plenty of small-scale three-dimensional vortex structures are present in the shear-layer of the TurBL-flu case and bridge the cavity from the leading edge to trailing edge. In the case of TurBL-ave, intense Mach waves radiate from the shear-layer and generate feedback compression waves, while no intense Mach wave and no intense feedback compression wave are generated in the TurBL-flu case. The dominant cavity tone in the TurBL-flu case has higher amplitude but exists in lower frequency than that of TurBL-ave case.

1. Introduction

Feedback-loop mechanism is the driving factor of self-sustained oscillations between shear-layer instability and acoustic forcing in supersonic open cavity flows. It could be described as three steps: (1) shear-layer is excited by the acoustic forcing of the feedback compression wave, which leads to shedding vortex and large-scale coherent structures; (2) shedding vortex convects downstream and impinges on the solid wall; and (3) a new feedback compression wave is generated, and it will propagate upstream and excite the shear-layer. Although the feedback-loop mechanism itself is well-established and accepted, some experimental phenomenon has not been well-understood[1-3], especially for high-speed compressible cavity flows. Questions underlying the basic physical phenomenon still remain and further investigations are needed.

In our previous work[4], feedback-loop mechanism is clearly verified using the visualization of one feedback loop. To be remarkable, we found that the feedback compression wave is generated by the reflection of Mach wave at the rear wall under the laminar-profiled inflow conditions. However, when fully turbulent inflows with presentence of random fluctuations and smaller-scaled vortex structures pass over the cavity, the behavior of the shear-layer and compression wave radiation may differ from those with laminar-profiled inflows. Understanding the behavior of the turbulent inflows could lead to significant contributions to the feedback-loop mechanism. The aim of this work is to clarify the effects caused by different turbulent inflows and to put insight into the physics of supersonic cavity flows.

2. Numerical Methods

(1) Flow Configures

Table 1 Parameters of the two cases

Cases	Ma	Re_D	*L/D*	*W/D*	θ	Inflow Profile	Turbulent fluctuation
TurBL-ave	2.0	10^5	2	0.6	0.02*D*	Turbulent	No
TurBL-flu							Yes

Supersonic flows over a cavity of *L/D*=2, *W/D*=0.6 are numerically studied, where *L* is the length of cavity, *W* is width of cavity, and *D* is the depth of cavity. Freestream Mach number is set to 2.0 and Reynolds number based on the cavity depth is set to 10^5. The momentum boundary-layer thickness (θ) at the leading lip is 0.02*D*. Two cases are conducted as shown below.

(2) Governing Equations and Numerical Algorithms

The governing equations are three-dimensional compressible Navier-Strokes equations in conservative form. Implicit large eddy simulations (ILES) are conducted, which rely on the numerical dissipation to dissipate high frequency turbulent energy. In order to meet the requirements of low dispersion and dissipation for computational aeroacoustics(CAA) and high-resolution simulations of turbulence flows, seventh-order weighted nonlinear compact scheme (WCNS)[5,6] is employed for the spatial derivatives. This numerical scheme had been validated to be effective for high-speed jet noise simulations.[7] The numerical fluxes are evaluated by the simple high-resolution upwind scheme (SHUS)[8] which is a family of advection-upstream-splitting-method (AUSM) type schemes. Viscous terms are evaluated by the sixth-order difference scheme. Alternate directional implicit symmetric Gauss-Seidel (ADI-SGS)[9] scheme is applied for time integration and Newton-like three sub-iterations are used to maintain second order temporal accuracy. The CFL number is approximately equal to 1.2.

(3) Grids and Boundary Conditions

The computational domain is shown in Fig. 1. The computational domain consists of inside the cavity region and upper cavity region. Structured grids are adopted and grid points are 213x211x150 in the inside cavity region, 488x177x150 in the upper cavity region, respectively. The total number of grid points is approximate 19.7 millions. The length from inflow boundary to the cavity leading lip is equal to 1.5*D*, and 4*D* is extended from trailing lip to outflow boundary. A distance of 4*D* is extended in the vertical direction and no buffer region is set because of supersonic freestream. In the spanwise direction, 150 points are equally distributed within the total length of 0.6*D*. The grids are refined at near wall region. The values of Δx^+, Δy^+, Δz^+ are 4.0, 0.8 and 8.0 respectively at the cavity leading lip. Inside the cavity, the largest grid spacing is constrained by Δy^+_{max}=24, Δx^+_{max}=24, Δz^+_{max}=8. Fine grids are used for the upstream region and inside cavity region for accurate simulation of the resolution of oncoming turbulent boundary-layer and the instable shear-layer

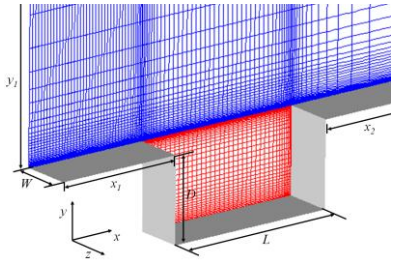

Fig. 1 Computational grids (shown every other five points)

No-slip adiabatic wall boundary condition is imposed at all the wall boundaries. Zero-gradient pressure condition is employed at the outflow, and periodical boundary condition is imposed in the spanwise direction. Recycling and rescaling technique[10] is adopted for the simulation of zero-pressure-gradient flat plate in the purpose of generation of a fully turbulent inflow. The results are validated in Fig.2 and Fig. 3.

The mean streamwise velocity profile in a semi-logarithmic plot using Van Driest transformation is shown in Fig. 2, which indicates the profile agrees well with theoretical formulation. Three components of velocity fluctuations in the turbulent boundary layer are compared with direct numerical simulation(DNS) conducted by Pirozzoli et al[11], in which Mach number equals to 2 and Re_σ is set to1.74x10^4. While in our simulation the Re_σ equals 2.0x10^4 which is slightly different from the DNS. The comparison shows the results of ILES simulation agree well with DNS and the turbulent inflow is adoptable for the simulation of supersonic cavity flow.

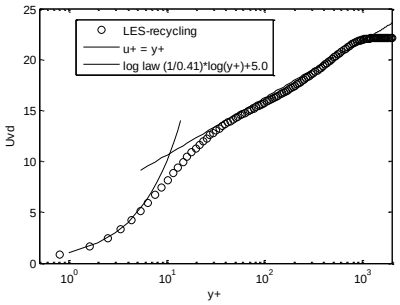

Fig. 2 Mean streamwise velocity profile of turbulent boundary layer of zero-pressure-gradient flat plate

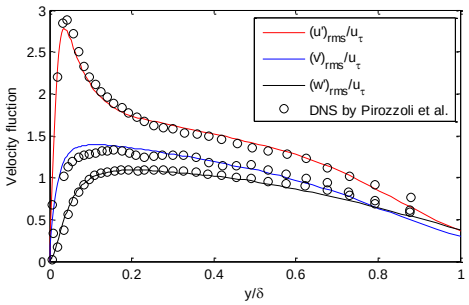

Fig. 3 Velocity fluctuations in one boundary layer thickness of zero-pressure-gradient flat plate

3. Results and Discussions

In the present study, the analysis is mainly focused on three aspects: 1) mean flowfields; 2) the behavior of the shear-layer and compression wave radiation, and 3) pressure spectrum of cavity tones.

(1) Mean Flowfields

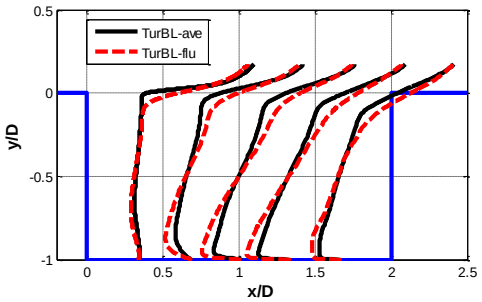

Fig. 4 Mean streamwise velocity profiles at the internal cavity

The mean streamwise velocity profiles at the internal cavity appear in Fig. 4. The profiles near the bottom wall indicate that the recirculation flow of the TurBl-flu case has higher speed than that of the TurBL-ave case. In the shear-layer region the streamwise velocity profiles of the TurBL-ave case are steeper than the other case, especially in the region near leading edge.

The contours of turbulence kinetic energy appear in Fig. 6. High values are found near the leading edge for the TurBL-flu case which implies rapid turbulent mixing at this region. Nonzero values are present in the oncoming flow since fully turbulent inflow condition is imposed at upstream. For the TurBL-ave case, high values are observed near the trailing edge and almost zero values are present in oncoming upstream.

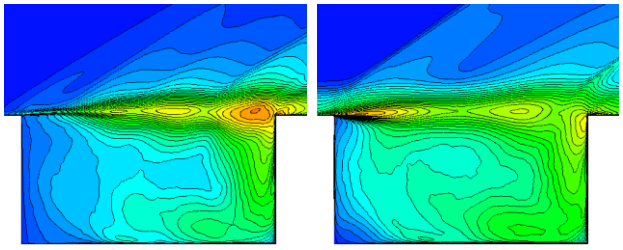

(a) TurBL-ave case (b) TurBL-flu case

Fig. 5 Contours of turbulence kinetic energy

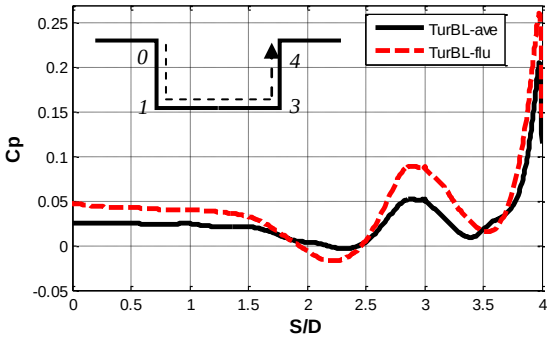

Fig. 6 Mean pressure coefficient distributions

The mean pressure coefficient distributions of the two cases are shown in Fig. 6. The mean flowfield of the TurBL-flu case has larger pressure coefficients at the right bottom corner and trailing-edge lip, which is supposed to be caused by higher speed flow injection flow from trainging edge and impingement at righ bottom corner, as illustrated in Fig. 4.

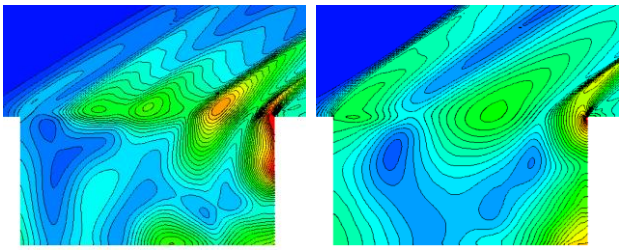

(a) TurBL-ave case (b) TurBL-flu case

Fig. 7 Contours of pressure fluctuation

The distributions of pressure fluctuation appear in Fig. 7, in which the contours are much different from each other. The TurBL-ave case has larger and higher values of pressure fluctuation near the trailing edge of the cavity, and has smaller and lower values near the leading edge. The TurBL-ave case has several peaks in the region from leading edge to trailing edge, while the TurBL-flu case only has one larger high pressure fluctuation region approximately at the mid of the cavity. These differences are caused by the much different behavior of shear-layer in the two simulation cases, which is discussed later.

(2) The Behavior of Shear-layer and Compression Wave Radiation

The behavior of shear-layer in cavity flows is an important clue for revealing the physical mechanism of self-sustained oscillations. In the two cases, the behavior of the shear-layer significantly differs from each other due to the difference in fluctuation components. The isosurface of the second invariant of velocity gradient tensors and the spanwise-averaged vorticity magnitude of an instantaneous flowfield is shown in Fig. 8 and Fig. 9, respectively.

Since the inflow of the TurBL-ave case does not contain turbulent fluctuations, the oncoming wall boundary-layer is dominated by two-dimensional characteristic without the presence of small-scaled vortex structures before it passes over the cavity. After the shear-layer separates from the leading edge, three-dimensional characteristic grows owning to K-H instability. In Fig. 8(a) a bulk of three-dimensional vortices is observed in the shear-layer near mid of the cavity, and a larger one exists near the trailing edge of the cavity. Although the vortices in the shear-layer are three-dimensional, highly two-dimensional characteristic is observed in spanwise direction by the visualization of spanwise-averaged vorticity magnitude in Fig. 9(a). Two shedding vortices are clearly observed. The scales of the vortices are comparable to the thickness of the shear-layer.

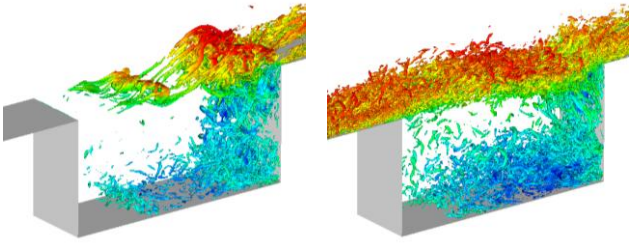

(a) TurBL-ave case (b) TurBL-flu case

Fig. 8 Isosurface of the second invariant of velocity gradient tensors ($Q_{2nd}=(U_{\infty}/\sigma)^2$)

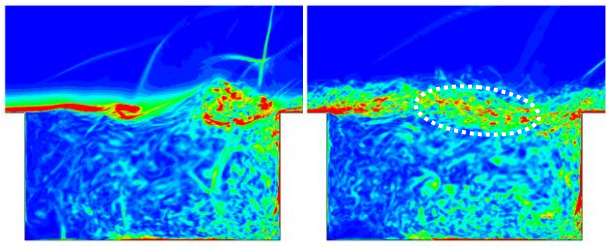

(a) TurBL-ave case (b) TurBL-flu case

Fig. 9 Contours of vorticity magnitude of spanwise-averaged flowfields

However, the behavior of the shear-layer in the TurBL-flu case is much different. As shown in Fig. 8(b), plenty of small-scale vortex structures are present not only in the oncoming stream but also in the shear-layer. The small-scale vortex structures consist of the shear-layer and bridge the cavity from the leading edge to the trailing edge. No clear large-scale coherent structure is observed in the shear-layer. In Fig. 9(b) contours of spanwise-averaged vorticity of the TurBL-flu case are shown, which indicates that the spanwise two-dimensional characteristic is weak. One large-scale vortex structure is observed near the trailing edge as marked by the white dot line. Many small-scale vortex structures are present near the right rear wall for the both cases because massively vortices inject into the cavity and become parts of recirculation flows.

In order to investigate the spreading rate of the shear-layer, vorticity boundary-layer thickness is adopted. The distribution of vorticity boundary-layer thickness is shown in Fig. 10 from leading edge to the trailing edge of the cavity. It indicates that the shear-layer of the TurBL-flu case grows rapidly from the leading edge to the region 0.5D from leading edge, and then the spreading rate slightly decreases but also at high value. However, the shear-layer of the TurBL-ave case has a small growth rate from the leading edge to the region approximately 0.3D from leading edge, and then grows with a high spreading rate. The vorticity boundary-layer thickness decreases near the trailing edge because of the impingement of shear-layer on the rear wall of the cavity.

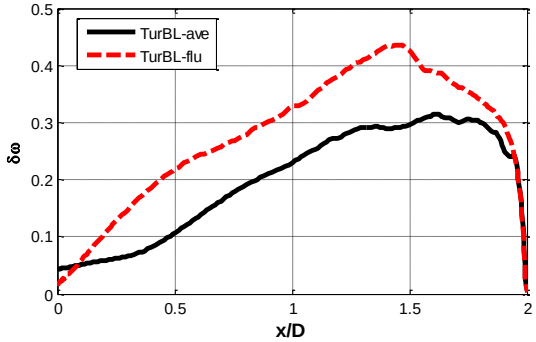

Fig. 10 The resolution of vorticity boundary layer thickness from leading edge to the trailing edge

The compression waves are captured by the absolute value of density gradient, which is shown as contour surface in Fig 11 coupling with visualization of positive values of Q_{2nd} as black contour lines. The category of compression waves in supersonic cavity had been summarized in our previous work.[1] As shown in Fig. 11(a), compression waves III^+ and compression waves III^- are

Mach waves in the upper cavity region and internal cavity region, respectively. Compression wave I and II are shock waves generated at the leading edge and trailing edge, and compression waves IV is feedback compression waves traveling toward front wall. Compression wave V and compression wave VI are generated by the reflection of feedback compression wave at the front wall and bottom wall, respectively. Detailed discussions about their features could refer to our previous work.[1]

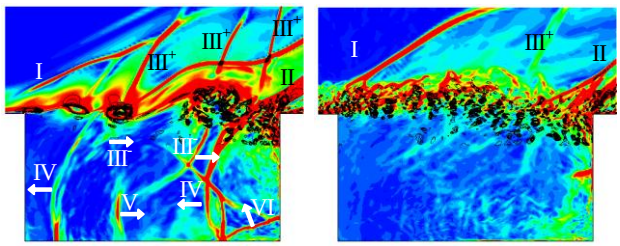

(a) TurBL-ave case (b) TurBL-flu case

Fig. 11 Compression wave radiation of a instantaneous flow (background contour surfaces are absolute values of density gradient; black contour lines are the second invariant of velocity gradient tensors)

Here we mainly focused on the discussion of Mach wave radiation, which is one of distinguishing features in supersonic cavity flows. As we known, Mach wave radiation occurs when the difference between the freestream velocity and the shear-layer convective velocity exceeds the local sound speed. Both sides of shear-layer could radiate Mach wave. In our previous work[1], we proposed that the feedback compression wave is generated by the reflection of Mach wave at the rear wall when the laminar-profiled inflow condition is imposed. In the present study, whether Mach wave reflection plays a crucial role in supersonic cavity flows is discussed.

In Fig. 11(a), Mach wave radiation in both sides of shear-layer is observed to be traveling with the shedding vortex. As time goes, the Mach wave inside the cavity reaches at the rear wall, and a clear reflection is observed which leads to a new feedback compression wave. This is similar to our previous simulation for laminar-profiled cases. However, no intense Mach wave radiates at the region inside the cavity from the shear-layer in the simulation of the TurBL-flu case. Instead, many weak Mach waves periodically radiate from the shear-layer but no clear reflection is observed near the rear wall. Moreover no intense feedback compression wave is observed inside the cavity, but the cavity tones exist in this case as in the pressure spectra shown later.

The different characteristic in Mach wave radiation is related to the different behavior of shear-layer as discussed above. If the supersonic convective shear-layer consists of plenty of small-scale vortex structures and has highly three-dimensional characteristic, the Mach waves radiated from the shear-layer may become weaker. The simulation of the TurBL-flu case demonstrates that Mach wave does not play a critical role to feedback-loop mechanism when the shear-layer is fully turbulent. But self-sustained oscillations are observed and the deriving mechanism on generation of feedback compression remains unclear.

(4) Cavity Tones

The spectra of pressure fluctuations at the mid-point of the front wall are shown in Fig. 12. First, the amplitudes of dominant cavity tone are different. The TurBL-flu case has larger amplitude for dominant cavity tone than that of the other case. The reason is probably related to more and higher-speed massively injection. As illustrated in Fig. 4 and Fig. 10, the TurBL-flu case has higher-speed recirculation flows at the internal cavity, and the shear-layer has larger spreading rate from the leading edge to the trailing edge, which lead to more mass flows inject into the cavity from the trailing edge and impinge on the right bottom corner. Second, the frequencies of the dominant cavity tone are different. The second mode at lower frequency is the dominant cavity tone in the TurBL-flu case, while the forth one in the TurBL-ave case. The cavity tones are greatly related to the behavior of the shear-layer.

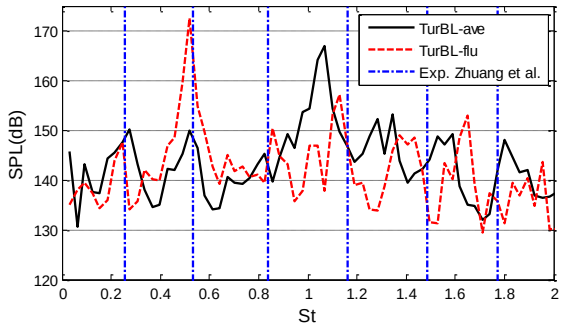

Fig. 12 Pressure spectra at the mid-point of the cavity front wall

The spectra are compared with the experiment conducted by Zhuang et al.[12] on Mach 2 flows over a cavity with length-to-depth (L/D) ratio of 2. The Reynolds number based on the depth of the cavity and the momentum boundary-layer thickness is $5.4*10^5$ and $1.8*10^4$, respectively. The peak values of the cavity tones in the experiment are plot in dash-blue line in Fig. 12, and the second mode is the dominant cavity tone. The comparison shows that the simulation of the TurBL-flu case matches well with experimental results.

4. Conclusion

The effects of turbulent inflow condition on feedback-loop mechanism are numerically studied by implicit large-eddy simulations of supersonic flows over a cavity under two turbulent-boundary-layer-profiled inflow conditions with fluctuations (TurBL-flu case) and without fluctuations (TurBL-ave case). Results show that higher-speed recirculation flows and high pressure distributions are observed in the TurBL-flu case. The behaviors of the shear-layer in these two cases are much different. Two-dimensional shedding vortices in spanwise are clearly observed in the shear-layer of the TurBL-ave case, while plenty of small-scale three-dimensional vortex structures are present in the shear-layer of the TurBL-flu case and bridge the cavity from the leading edge to trailing edge. In the case of TurBL-ave, intense Mach waves radiate from the shear-layer and generate feedback compression waves, while no intense Mach wave and no intense feedback compression wave are generated in the TurBL-flu case. The dominant cavity tone in the TurBL-flu case has higher amplitude but exists in lower frequency than that of TurBL-ave case.

Bibliography

(1) Ünalmis, Ö. H., Clemens, N. T., and Dolling, D. S.,

"Experimental Study of Shear-Layer/Acoustics Coupling in Mach 5 Cavity Flow," AIAA Journal, Vol. 39, No. 2, 2001, pp. 242-252.

(2) Vikramaditya, N. S., and Kurian, J., "Pressure Oscillations from Cavities with Ramp," AIAA Journal, Vol. 47, No. 12, 2009, pp. 2974-2984.

(3) Heller, H. H., and Bliss, D. B., "The Physical Mechanism of Flow-induced Pressure in Cavities and Concepts for Their Suppression," AIAA Paper 1975-491, Mar. 1975

(4) Li, W., Nonomura, T., Oyama, A, and Fujii, K. "LES Study of Feedback-loop Mechanism of Supersonic Open Cavity Flows," AIAA Papers, AIAA 2010-5112

(5) Nonomura, T., and Fujii, K., "Effects of Difference Scheme Type in High-order Weighted Compact Nonlinear Schemes," Journal of Computational Physics. Vol. 228, 2009, pp. 3533–3539.

(6) Nonomura, T., Iizuka, N., and Fujii, K., "Freestream and Vortex Preservation Properties of High-order WENO and WCNS on Curvilinear Grids," Computers and Fluids, Vol. 39, 2010, pp. 197–214.

(7) Nonomura, T., and Fujii, K., "Computational Analysis of Characteristics of Mach Wave Sources in Supersonic Free-jets," AIAA 2009-16, Jan. 2009.

(8) Shima, E. and Jounouchi, T., "Role of CFD in Aeronautical Engineering (No. 14) -AUSM type Upwind Schemes," Proceedings of the 14th NAL Symposium on Aircraft Computational Aerodynamics, National Aeroautical Laboratory, Tokyo, 1997, pp. 7-12.

(9) Nishida, H., and Nonomura, T., "ADI-SGS Scheme on Ideal Magnetohydrodynamics," Journal of Computational Physics. Vol. 228, 2009, pp. 3182–3188.

(10) Urbin, G., and Knight, D., "Large-Eddy Simulation of a Supersonic Boundary Layer Using and Unstructured Grid," AIAA Journal, Vo.39, No.7, 2001, pp.1288-1295.

(11) Pirozzoli, S., Bernardini, M., Grasso, F., "Characterization of coherent vortical structures in a supersonic turbulent boundary layer," Journal of Fluid Mechanics, Vol 613, 2008, pp. 205–231.

(12) Zhuang, N., Alvi, F. S., and Shih, S., "Another Look at Supersonic Cavity Flows and Their Control," AIAA Paper 2005-2803, May 2005.